

Enzymes

Switching the Switch: Ligand Induced Disulfide Formation in HDAC8

Niklas Jänsch,^[a] Wisely Oki Sugiarto,^[a] Marius Muth,^[a, b] Aleksandra Koprancovic,^[a] Charlotte Desczyk,^[a] Matthias Ballweg,^[a] Frank Kirschhöfer,^[b] Gerald Brenner-Weiss,^[b] and Franz-Josef Meyer-Almes^{*[a]}

Abstract: Human histone deacetylase 8 is a well-recognized target for T-cell lymphoma and particularly childhood neuroblastoma. PD-404,182 was shown to be a selective covalent inhibitor of HDAC8 that forms mixed disulfides with several cysteine residues and is also able to transform thiol groups to thiocyanates. Moreover, HDAC8 was shown to be regulated by a redox switch based on the reversible formation of a disulfide bond between cysteines Cys₁₀₂ and Cys₁₅₃. This study on the distinct effects of PD-404,182 on HDAC8 re-

veals that this compound induces the dose-dependent formation of intramolecular disulfide bridges. Therefore, the inhibition mechanism of HDAC8 by PD-404,182 involves both, covalent modification of thiols as well as ligand mediated disulfide formation. Moreover, this study provides a deep molecular insight into the regulation mechanism of HDAC8 involving several cysteines with graduated capability to form reversible disulfide bridges.

Introduction

Human histone deacetylase 8 (HDAC8) belongs to the histone deacetylase family containing 11 human isoenzymes that are subdivided into four classes. Contrary to most other isoenzymes, HDAC8 is not a member of multi-protein complexes, but rather interacts with only a handful of established other mostly cytosolic proteins.^[1–11] HDAC8 is a validated target for several types of cancer including T-cell lymphoma and childhood neuroblastoma.^[12–18] In the effort to discover new potent and selective non-hydroxamate inhibitors of HDAC8, we identified PD-404,182 in a medium-scaled compound screening campaign.^[19] Further studies on the mode of protein-inhibitor interaction revealed that PD-404,182 is a covalent modifier of HDAC8, forms mixed disulfides and transforms thiol groups into thiocyanates.^[20] In a further study we found that HDAC8 is

regulated by a redox switch involving cysteines Cys₁₀₂ and Cys₁₅₃.^[21] H₂O₂ was shown to oxidize the protein resulting in a disulfide bridge between these cysteines and concomitant reversible loss of enzyme activity.

Considering protein–inhibitor interactions, there are only very few examples of drug-like small molecules that are able to induce disulfide bond formation. Mathieu et al. showed that thiram, a neurotoxic disulfide-containing dithiocarbamate compound inhibits brain glycogen phosphorylase through the formation of an intramolecular disulfide bond between Cys₃₁₈ and Cys₃₂₆, known to be a redox-switch that prevents the allosteric activation of the enzyme by AMP.^[22,23] The proposed mechanism consists of the reaction of thiram with a cysteine thiol leading to a mixed disulfide followed by the formation of an intramolecular disulfide bond with a vicinal cysteine residue. Another example describes the inactivation of an arginine phosphatase by a seleno-compound that induces an intramolecular disulfide bond between two adjacent active site cysteines via an unclear mechanism.^[24] Moreover, Yang et al. reported an example for the bile salt-induced isomerization from intramolecular to an intermolecular disulfide bridge between two subunits of a transmembrane transcription factor, which directly activates the virulence cascade of *Vibrio cholerae* by a host signal molecule.^[25]

In this study, we show that PD-404,182 alters the activity of HDAC8 through the formation of an intramolecular disulfide bond between Cys₁₀₂ and Cys₁₅₃. Thus, PD-404,182 acts as a molecular trigger that operates this redox switch resulting in the inactive oxidized form of HDAC8. Moreover, PD-404,182, unlike oxidation by H₂O₂, induces additional disulfide bridges in HDAC8. The formation of a distinct disulfide bond between Cys₂₇₅ and Cys₃₅₂ also has strong impact on HDAC8 activity,

[a] N. Jänsch, W. O. Sugiarto, M. Muth, A. Koprancovic, C. Desczyk, M. Ballweg, Prof. Dr. F.-J. Meyer-Almes
Department of Chemical Engineering and Biotechnology
University of Applied Sciences Darmstadt, Stephanstraße 7
64295 Darmstadt (Germany)
E-mail: franz-josef.meyer-almes@h-da.de

[b] M. Muth, F. Kirschhöfer, Dr. G. Brenner-Weiss
Institute of Functional Interfaces (IFG)
Karlsruhe Institute of Technology (KIT), Hermann-von-Helmholtz Platz-1
76334 Eggenstein-Leopoldshafen (Germany)

Supporting information and the ORCID identification number(s) for the author(s) of this article can be found under:
<https://doi.org/10.1002/chem.202001712>.

© 2020 The Authors. Published by Wiley-VCH GmbH. This is an open access article under the terms of Creative Commons Attribution NonCommercial License, which permits use, distribution and reproduction in any medium, provided the original work is properly cited and is not used for commercial purposes.

thus acting as allosteric regulative residues besides the already known Cys₁₀₂/Cys₁₅₃ redox switch at the active site. These results provide strong evidence for a complex and until now unknown redox-based regulation mechanism of HDAC8 involving more than one disulfide bridge.

Results and Discussion

In a previous study, we identified PD-404,182 as a potent and selective HDAC8 inhibitor.^[19] By using time resolved HPLC-MS/MS, we also explained the exact mechanism of PD-404,182 decomposition in aqueous solution and subsequent mixed disulfide formation of various cysteines in HDAC8.^[20] PD-404,182 decomposes quickly into the corresponding sulfenamide, which forms mixed disulfides with cysteine residues for example, in HDAC8. Another adjacent cysteine can react with this intermediate by forming an intramolecular disulfide bridge between the involved cysteine side chains (Figure 1). In the light of our previous study about the redox regulation of HDAC8^[21] we questioned whether PD-404,182 is able to induce a disulfide bridge between Cys₁₀₂ and Cys₁₅₃ of HDAC8 through its mixed disulfide and thus acts as a molecular trigger of the corresponding redox switch that regulates the enzyme activity of HDAC8.

Structural and sequence alignments

HDAC8 contains ten cysteines, eight of them are in proximity to each other and therefore able to form disulfides in general (Figure 2). To clarify if these eight cysteines are conserved through the other HDAC isoenzymes we made a structural alignment of HDACs 1–8 (Figure 3). Additionally, we made sequence alignments including HDAC8 homologues from different species (Figure S1). As discussed in the context of redox regulation of HDAC8,^[21] Cys₁₀₂ is conserved in all class I HDACs and Cys₁₅₃ is conserved throughout all other HDACs. Also, both cysteines are conserved in all HDAC8 homologues from different species. This implies a fundamental role for Cys₁₀₂ and Cys₁₅₃ for HDAC and particularly HDAC8 function.

Taking a glance at the crystal structure of HDAC8 (PDB-ID: 1T69) reveals three additional pairs of cysteines (Cys₁₂₅/Cys₁₃₁, Cys₂₇₅/Cys₃₅₂ and Cys₂₄₄/Cys₂₈₇) in proximity (3.6–11.9 Å between the corresponding sulfur atoms) potentially enabling the formation of further disulfide bonds.

Cys₁₂₅ and Cys₁₃₁ are unique for HDAC8 and not present in other human isoenzymes. Interestingly, these cysteines are conserved in ortholog HDAC8 sequences from other species with a slightly difference for HDAC8 from *Schistosoma mansoni*

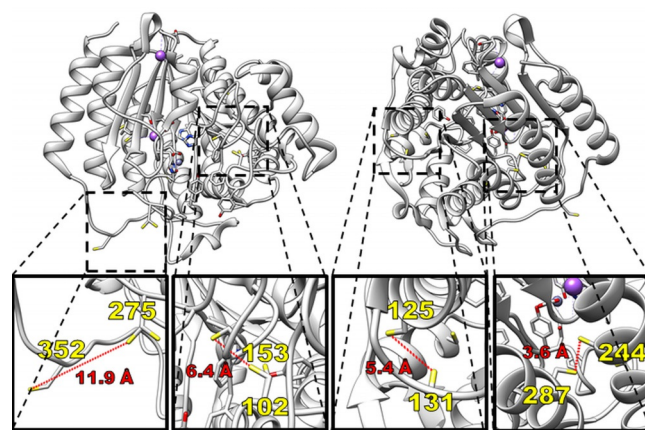


Figure 2. Structural overview of the investigated Cysteine pairs in HDAC8 (PDB-ID: 1T64).

(smHDAC8). The possible disulfide bond between Cys₂₇₅ and Cys₃₅₂ is interesting because Cys₂₇₅ is only conserved in HDACs from class I and Cys₃₅₂ is unique to HDAC8. Both cysteines are conserved in HDAC8 homologues except for smHDAC8. The same observation could be made for the last putative disulfide bond. Cys₂₈₇ is conserved in class I HDACs and Cys₂₄₄ is unique to HDAC8. Both are conserved in HDAC8 homologues and not present in smHDAC8. To rationalize the reactivity of each disulfide pair, we calculated the pK_a value and the solvent accessible surface area (SASA) of each mentioned cysteine in HDAC8 (Figure S7). A plot of pK_a values against the logarithmic SASA reveals that Cys₁₅₃ has the lowest pK_a value. Therefore, the disulfide bond between Cys₁₀₂ and Cys₁₅₃ should be the most reactive one. Cys₂₇₅ and Cys₃₅₂ are the most accessible cysteines in HDAC8. We conclude that the reactivity of this disulfide bond is mainly driven by accessibility. Cys₁₂₅ and Cys₁₃₁ range between the two other disulfide bonds in terms of both, reactivity and accessibility. Cys₂₄₄ and Cys₂₈₇ are the most buried ones with the highest pK_a value and thus lowest theoretical reactivity. With these characteristic values it seems remarkable that these cysteines can undergo disulfide formation. Nevertheless, there exists a crystal structure where precisely these cysteines are interconnected by a disulfide bridge (PDB: 1VKG). The alignments and the reactivity/accessibility calculations suggest that HDAC8 consists of a unique pattern of cysteines not found in other HDACs and therefore provides an excellent basis for utilizing redox based regulation mechanisms to achieve isoenzyme selectivity through targeted cysteine oxidation or alkylation.

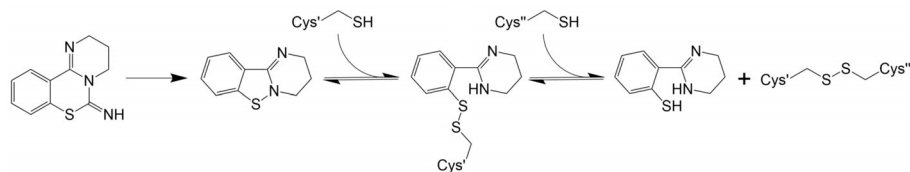


Figure 1. Mechanism of PD-404,182 induced disulfide formation.

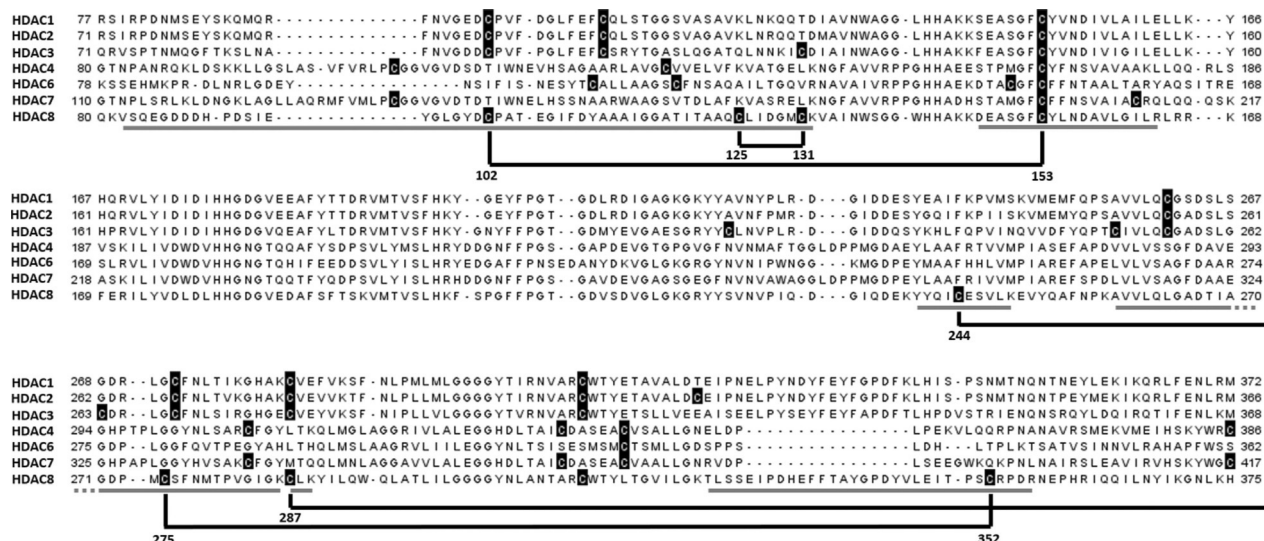


Figure 3. Structural alignment of HDAC1, 2, 3, 4, 6, 7 and 8. Cysteines are marked in black and disulfides in HDAC8 relate to black lines. Theoretical peptide fragments are indicated with grey bars beneath the alignment. Numbers on the left and right edge indicates the amino acid numbers corresponding to following PDB IDs: HDAC1 (4BKX), HDAC2 (5IWG), HDAC3 (4A69), HDAC4 (2VQJ), HDAC6 (5W5K), HDAC7 (3C0Z), HDAC8 (1T69).

Electrophoretic mobility shift assays (EMSA)

In our previous study, the H_2O_2 dependent formation of a single disulfide bond between Cys₁₀₂ and Cys₁₅₃ was demonstrated by using a non-reductive electrophoretic mobility shift assay (EMSA).^[21] The difference in the mobility shift of the protein on a non-reductive SDS-PAGE depends predominantly on the amino acid distance between the two covalently bound cysteines. Thus, it should be possible to clarify if PD-404,182 is inducing one or more disulfide bonds.

At first, the EMSA was performed with the HDAC8_{wt} enzyme (Figure 4A). HDAC8 was incubated with different concentrations of PD-404,182. Afterwards, an aliquot of the reaction mixture was removed and conducted to an enzyme activity assay. The rest of the reaction mixture was precipitated with trichloroacetic acid (TCA), the supernatant was removed, and the protein precipitate was resuspended in non-reducing sample buffer with the addition of 50 mM NEM. The alkylation of the protein is necessary to prevent nascent thiols from artificial oxidation with oxygen whilst the following non-reductive SDS-PAGE. The concentration dependent inhibition of the wild type enzyme shows a dependence between loss in enzyme activity (left bar) and disulfide bond formation (right bar) (Figure 4A). The first band shift is identified as the disulfide bond between Cys₁₀₂ and Cys₁₅₃ according to our previous study on the redox switch of HDAC8.^[21] Therefore, PD-404,182 is mainly regulating the enzyme activity of HDAC8 by triggering its redox switch. Interestingly, more disulfides occur at higher concentrations of PD-404,182. The appearance of additional bands in the EMSA experiment enabled the identification of three distinct oxidative species of HDAC8 shifted to apparent lower molecular weights on the gel (Figure 4A). As mentioned before, the amino acid distance is the key feature that determines divergent migration behavior in an EMSA gel. The two additional oxidative species are supposed to be disulfide bonds between

Cys₂₇₅/Cys₂₄₄ and Cys₂₇₅/Cys₃₅₂. The distance between Cys₁₂₅ and Cys₁₃₁ seems too small to expect a visible difference in an EMSA gel without the utilization of special polymer-based alkylation agents like poly (ethylene glycol)-maleimides as electrophiles.

To confirm the hypothesis that the first disulfide bond formed upon the addition of PD-404,182 is between Cys₁₀₂ and Cys₁₅₃ further EMSA experiments were carried out with the double mutant enzyme HDAC8_{C102S/C153S}. In contrast to our expectations, the double mutant enzyme is not fully resistant to PD-404,182. Surprisingly, the enzyme activity drops to about 50% compared with the control (Figure 4B). This behavior led us to the assumption that HDAC8 contains at least one allosteric regulating disulfide bond beyond the redox switch between Cys₁₀₂ and Cys₁₅₃. To dissect this unexpected behavior, three constructs were generated on the basis of the HDAC8_{C102S/C153S} vector, where in each case one additional pair of cysteines is changed to serine, namely HDAC8_{C102S/C153S/C125S/C131S}, HDAC8_{C102S/C153S/C244S/C287S} and HDAC8_{C102S/C153S/C275S/C352S}. Interestingly, the yield of recombinant protein varies dramatically between the mutant variants. The EMSA experiments with these multiple mutant variants of HDAC8 clearly shows that the HDAC8_{C102S/C153S/C275S/C352S} variant retains nearly full enzyme activity in the presence of even the highest used concentrations of PD-404,182 (Figure 4C). Therefore, we conclude that the formation of a disulfide bond between Cys₂₇₅ and Cys₃₅₂ is regulating the enzyme activity in an allosteric manner. The EMSA results for the HDAC8_{C102S/C153S/C125S/C131S} and HDAC8_{C102S/C153S/C244S/C287S} mutant variants are shown in Figure S8.

The enzyme activity of both mutant variants drops below 50% residual activity at the highest concentrations of PD-404,182. This underlines the assumption that the disulfide bond between Cys₂₇₅ and Cys₃₅₂ is regulating the enzyme activity because this disulfide bond is still present in these mutants.

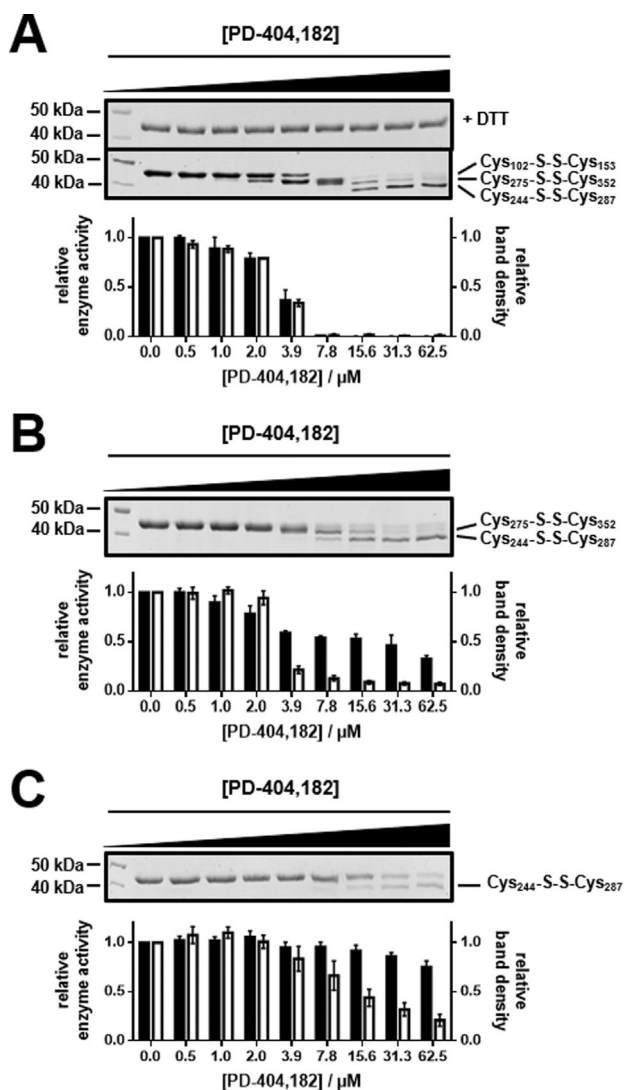


Figure 4. Electrophoretic mobility shift assay (EMSA) showing disulfide bond induced loss of enzyme activity. A) EMSA for the HDAC8_{wt}, B) HDAC8_{C102S/C153S}, C) HDAC8_{C102S/C153S/C275S/C352S} enzyme.

Moreover, we were able to show that the disulfide bond between Cys₁₂₅ and Cys₁₃₁ is not observable in the EMSA, because the HDAC8_{C102S/C153S/C125S/C131S} mutant variant behaves similarly to the HDAC8_{C102S/C153S} variant and shows two distinct shifts on the EMSA gel, which correspond to the disulfide bonds between Cys₂₄₄/Cys₂₈₇ and Cys₂₇₅/Cys₃₅₂.

To test for reversibility of disulfide bond formation and verify that the observed mobility shift on the EMSA gel occurs exclusively throughout disulfide formation, the EMSA was performed with the wild type enzyme and PD-404,182 with subsequent addition of 50 mM β-ME. No band shifts can be observed implying that all changes on EMSA must be due to disulfide formation. In addition, it was shown in our previous study that inhibition of HDAC8 enzyme activity through PD-404,182 is reversible after the addition of TCEP and β-ME.^[20]

HPLC-MS/MS confirmation of induced disulfide bridges

To confirm the formation of the proposed regulating disulfide bonds, we performed high-resolution HPLC-MS/MS experiments. Therefore, we primarily induced the disulfide bonds in HDAC8_{wt} by the reaction with PD-404,182 under comparable conditions and the same inhibitor/enzyme ratio (25-fold excess of inhibitor) corresponding to the highest concentration in the EMSA (Figure 4). A solvent control without inhibitor was carried out simultaneously to ensure that the generated disulfides are specific for the treatment. After treatment the reaction was immediately stopped by TCA precipitation and guanidine denaturation of HDAC8_{wt} followed by iodoacetamide alkylation. Subsequently, samples were cleaved into peptides using trypsin under non-reductive conditions to obtain treatment dependent disulfide bonds. Possible disulfide shuffling during the digestion process was prevented by mild buffer conditions, 10 mM ammonium bicarbonate pH 8.0, and relatively short digestion times of three hours. To ensure the accuracy of the acquired results, two independent replicates were made for the treated and control samples (Figure S2). The chromatographic separation of the digested samples already revealed distinct differences in their composition between treated and non-treated samples (Figure 5A). Beside the decreasing total ion

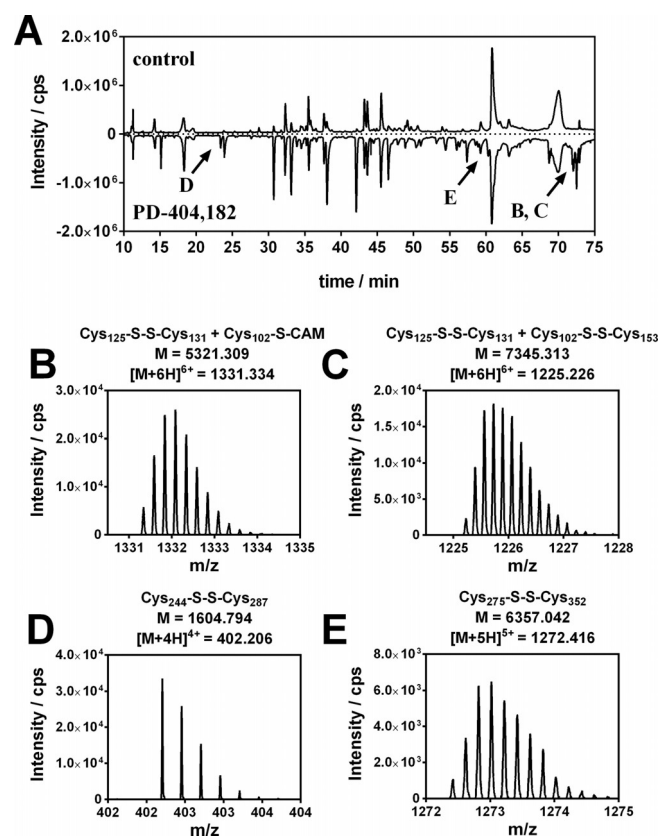


Figure 5. HPLC-MS/MS analysis of disulfide linked tryptic HDAC8 fragments. A) HPLC chromatogram of the untreated and PD-404,182 treated HDAC8 samples. B) Mass spectra for the Cys₁₂₅-S-S-Cys₁₃₁-S-CAM, C) Cys₁₂₅-S-S-Cys₁₃₁ + Cys₁₀₂-S-S-Cys₁₅₃, D) Cys₂₄₄-S-S-Cys₂₈₇, E) Cys₂₇₅-S-S-Cys₃₅₂ peptide fragment.

current (TIC) of peptide fragments with alkylated cysteines and increasing intensity of cyanlated cysteine fragments (not shown,^[20] for reference), the appearance of four distinct peaks in the treated sample is most noticeable as highlighted in Figure 5A. These new arising signals (5C, 5D and 5E) are not present in the control samples or clearly enriched in the treated samples (5B). For those signals the assigned masses match the theoretical masses of the four proposed disulfide linked peptides with an error below 2 ppm (Figure 5B-E, Table S1). The observed masses and isotopic distributions fit perfectly to the expected masses of the disulfide linked tryptic peptides Cys₁₂₅-Cys₁₃₁, Cys₁₂₅-Cys₁₃₂ + Cys₁₀₂-Cys₁₅₃, Cys₂₄₄-Cys₂₈₇ and Cys₂₇₅-Cys₃₅₂. To confirm the identity of these interlinked peptides, we acquired high resolution fragmentation spectra (Figures S3–S6). Because of the quadrupole ion selection prior to collision induced fragmentation only one peptide ion is observed and fragmented at a time. Therefore, several situations should be observable: 1) intermolecular linked tryptic peptides should generate N- and C-terminal fragmentation patterns specific for these two peptides, 2) disulfide linked fragment ions should occur due to favored fragmentation of the more fragile peptide bonds or 3) intramolecular linked fragments can be identified by the absence of carbamidomethyl (CAM) groups and a distinct mass difference of two protons as a result of the connected thiols. Also, the large size of such linked peptides, especially Cys₁₂₅-Cys₁₃₂ + Cys₁₀₂-Cys₁₅₃, can lead to internal fragmentations. In this work, we were able to clearly identify all four proposed disulfide bonds in HDAC8_{wt} induced by PD-404,182 on the basis of all the above-mentioned states (Figures S3–S6, Tables S2–5). The intramolecular and in proximity located disulfide bond between Cys₁₂₅-Cys₁₃₁ could be observed in several fragment ions, where the thiols show the absent hydrogens and CAM group. However, Cys₁₀₂ was modified by a CAM group in the same precursor ion. This was the only disulfide linked species, which was also observed in the untreated control sample (Figure S3 and S4, Tables S2 and S3). Considering that this disulfide bond is not observable in the EMSA, we hypothesize that this disulfide bond is easily build even in the absence of oxidizing agents. The other three disulfide linked peptides were exclusively observed in the treated samples. The precursor of Cys₁₀₂-Cys₁₅₃ shows a similar fragment pattern of the Cys₁₂₅-Cys₁₃₁ peptide in addition to the N- and C-terminal (b- and y-ion) fragments of the peptide, where Cys₁₅₃ is located. Only few Cys₁₀₂-Cys₁₅₃ linked fragments were identified, likely because of the large size of those peptides. Both, the N- and C-terminal fragmentations as well as several disulfide-linked fragment ions were identified in the Cys₂₄₄-Cys₂₈₇ and Cys₂₇₅-Cys₃₅₂ fragmentation spectra providing clear evidence for their existence. Overall, these data confirm the presence of all four disulfide linked peptides, especially Cys₁₀₂-Cys₁₅₃, Cys₂₄₄-Cys₂₈₇ and Cys₂₇₅-Cys₃₅₂, after treatment with a 25-fold excess of PD404,182.

Thermal shift assay provides insight into disulfide induced enzyme stabilization

As proven by EMSA and HPLC-MS/MS, the interaction between HDAC8 and PD-404,182 leads to several oxidized enzyme species. In general, it would be expected that the formation of disulfide bonds leads to protein stabilization. To elucidate the effect on increasing concentrations of PD-404,182 on the overall stability of HDAC8, thermal shift assays were performed using SYPRO orange dye on a real time PCR thermo cycler (Figure 6). To allow for a meaningful comparison, the concentrations of HDAC8 and PD-404,182 were the same as in the previous EMSA experiment (Figure 4). Considering that the fluorescence of SYPRO orange increases upon binding to exposed hydrophobic domains of the protein, the fluorescence signal can not only be used to detect thermal unfolding, but also changes in hydrophobic surface area due to conformational changes. Interestingly, at low concentrations of PD-404,182, ranging from 1 μM to 7.8 μM the melting temperature increases from 47 $^{\circ}\text{C}$ to about 51 $^{\circ}\text{C}$. This correlates with the first mobility shift on the EMSA, which is supposed to be the

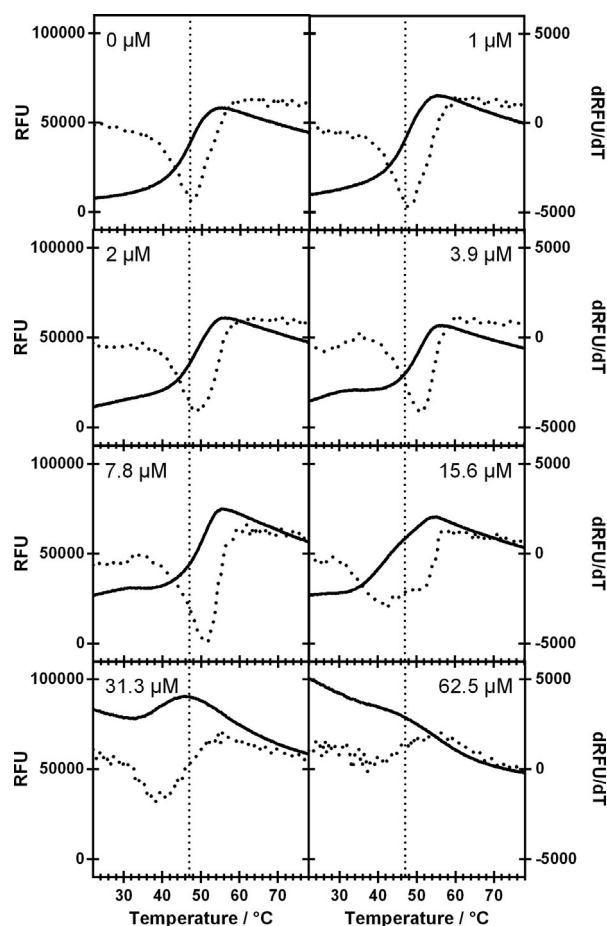


Figure 6. Thermal shift assay of HDAC8 incubated with various concentrations of PD-404,182. The black lines show the increase of SYPRO orange fluorescence upon thermal unfolding of HDAC8. The dotted lines represent the first derivatives of thermograms. Vertical dotted lines correspond to the melting point of the untreated control sample.

disulfide bond between Cys₁₀₂ and Cys₁₅₃, as well as the allosteric disulfide bond between Cys₂₇₅ and Cys₃₅₂ (Figure 4). The oxidation of these residues results in a thermodynamically stabilized and therefore favored conformation of the enzyme. At 15.6 μM of PD-404,182 a second inflection point is observed. The melting point of the stabilized protein disappears, and a second melting point occurs at about 40 °C. In the presence of the two highest concentration of PD-404,182 the melting point at elevated temperature disappears completely and only one transition at lower temperature (40 °C) remains visible. We conclude that very high concentrations of PD-404,182 inducing the formation of two additional disulfide bridges destabilize HDAC8 compared to its reduced form. The destabilization of the enzyme in the presence of the highest inhibitor concentrations correlates with a considerably elevated onset in the thermogram, which is indicative for a dramatic change in the hydrophobic surface area and tertiary structure of the peroxidized HDAC8 protein.

Conclusions

This study provides detailed insight into how PD-404,182 acts as a molecular trigger of intermolecular disulfide bond formation within HDAC8. We identified the disulfide bond between Cys₁₀₂ and Cys₁₅₃ as a main regulatory switch for enzyme activity after treatment with PD-404,182. Additionally, we were able to identify an allosteric regulating disulfide bond between Cys₂₇₅ and Cys₃₅₂, which inhibits HDAC8 activity to about 50% residual enzyme activity. A mutant HDAC8 variant, where those four cysteines are mutated to serine retains enzyme activity at the same concentration of PD-404,182. At higher concentrations of PD-404,182 all proposed four disulfides are formed. The findings were confirmed by tryptic digestion and mass analytics. Additionally, we verified that the oxidation of the disulfide bonds between Cys₁₀₂/Cys₁₅₃ and Cys₂₇₅/Cys₃₅₂ results in a thermodynamically stabilized protein and further oxidation results in a dramatic destabilization of the enzyme. The impact of oxidation on the overall HDAC8 structure is still unclear and needs further research.

Based on the knowledge gained in this study and the unique pattern of regulative disulfide bonds in HDAC8, we propose to develop covalent isoenzyme selective inhibitors that target the identified pairs of cysteines. Corresponding work is ongoing in our laboratory.

Experimental Section

Electrophoretic mobility shift assay (EMSA)

For the determination of ligand induced disulfide bond formation 2.5 μM wild type and mutant HDAC8 was treated with the indicated concentrations of PD-404,182 for 1 h at 30 °C in assay buffer (pH 8.0, 25 mM Tris, 75 mM KCl, 0.001% Pluronic F-68) in 50 μL reaction volume. Afterwards 10 μL were removed and diluted 1:100 in assay buffer and stored on ice until the activity assay was performed as described later. The remaining reaction mixture was treated with 10% TCA and protein precipitation was performed at –20 °C for 20 min with subsequent centrifugation at 18000 g for

10 min at 4 °C. Afterwards, the supernatant was removed and precipitate was dissolved in 30 μL alkylation buffer (pH 7.0) containing 150 mM NaCl, 20 mM NaH₂PO₄, 20 mM Na₂HPO₄, 5 mM EDTA, 50 mM NEM and 10 μL non-reducing Laemmli sample buffer (4x, pH 6.8) containing 250 mM Tris, 8% SDS, 40% glycerol, 0.02% bromophenol blue for 30 min at 30 °C with subsequent heat denaturation at 95 °C for 5 min. For the determination of the reversibility against reducing agents the precipitate was dissolved in alkylation buffer without NEM and 10 μL 4x Laemmli sample buffer with the addition of 200 mM DTT and conducted as listed above. Finally, 15 μL of the sample was subjected to SDS-PAGE and gels were stained with Coomassie brilliant blue solution.

Enzyme activity assay

For the determination of disulfide bond induced changes in enzyme activity 20 nM of the prior treated HDAC8 dilution was mixed with 20 μM Boc-Lys(trifluoroacetyl)-AMC as substrate in a black 96-well microtiter plate (Greiner) in assay buffer for 15 min at 30 °C. For the HDAC8_{C102S/C153S} mutant the substrate reaction was conducted for 1 h. After substrate conversion the reaction was stopped by the addition of 1.7 μM SATFMK and fluorescent AMC was released by the addition 0.4 mg mL⁻¹ trypsin. Relative fluorescent units were measured in a microplate reader at 450 nm ($\lambda_{\text{ex}} = 350 \text{ nm}$) and normalized to the untreated control.

Sample preparation for mass spectrometry

HDAC8_{wt} in storage buffer containing (pH 8.0, 150 mM KCl, 50 mM Tris, 25% glycerol, 1 mM TCEP) was buffer exchanged to 10 mM NH₄HCO₃ pH 8.0 with mini GPC column (self-packed Bio Gel-P6, Biorad) at 1020 g for 4 min. Buffer exchanged samples containing 25.5 μM HDAC8 were treated with no inhibitor and 25-fold excess (637 μM) PD-404,182 (TOCRIS) for 1 h at 30 °C followed by protein precipitation with 10% TCA (see EMSA section). Precipitated protein was resuspended in 10 mM NH₄HCO₃ containing 5 M guanidine and 10 mM iodoacetamide (Merck). Alkylation was performed at 22 °C for 20 min under exclusion of light followed by desalting with mini GPC columns. Samples were tryptic digested with 5 μg (50 ng μL^{-1}) in 10 mM NH₄HCO₃ activated trypsin sequencing grade (Promega) for 3 h at 37 °C and 550 rpm. Reaction was stopped by addition of 1% FA (VWR) and prior to injection centrifugated at 18000 g for 10 min. 10 μL Supernatant was used for HPLC-MS injection.

Acknowledgements

This work was supported by a fellowship of the Platform for PhD students of the Technical University of Darmstadt. The excellent technical support of Michael Schröder is gratefully acknowledged. Open access funding enabled and organized by Projekt DEAL.

Conflict of interest

The authors declare no conflict of interest.

Keywords: cysteine • HDAC8 • covalent inhibitors • redox switch • sulfenamides

- [1] N. Alam, L. Zimmerman, N. A. Wolfson, C. G. Joseph, C. A. Fierke, O. Schueler-Furman, *Structure* **2016**, *24*, 458–468.
- [2] F. Beckouët, B. Hu, M. B. Roig, T. Sutani, M. Komata, P. Uluocak, V. L. Katis, K. Shirahige, K. Nasmyth, *Mol. cell* **2010**, *39*, 689–699.
- [3] M. A. Deardorff, M. Bando, R. Nakato, E. Watrin, T. Itoh, M. Minamino, K. Saitoh, M. Komata, Y. Katou, D. Clark, K. E. Cole, E. de Baere, C. Decroos, N. Di Donato, S. Ernst, L. J. Francey, Y. Gyftodimou, K. Hirashima, M. Hullings, Y. Ishikawa, C. Jaulin, M. Kaur, T. Kiyono, P. M. Lombardi, L. Magnaghi-Jaulin, G. R. Mortier, N. Nozaki, M. B. Petersen, H. Seimiya, V. M. Siu, Y. Suzuki, K. Takagaki, J. J. Wilde, P. J. Willems, C. Prigent, G. Gillissen-Kaesbach, D. W. Christianson, F. J. Kaiser, L. G. Jackson, T. Hirota, I. D. Krantz, K. Shirahige, *Nature* **2012**, *489*, 313–317.
- [4] K. L. Durst, B. Lutterbach, T. Kummalu, A. D. Friedman, S. W. Hiebert, *Mol. Cell. Biol.* **2003**, *23*, 607–619.
- [5] J. Gao, B. Siddoway, Q. Huang, H. Xia, *Biochem. Biophys. Res. Commun.* **2009**, *379*, 1–5.
- [6] D. E. Olson, N. D. Udeshi, N. A. Wolfson, C. A. Pitcairn, E. D. Sullivan, J. D. Jaffe, T. Svinkina, T. Natoli, X. Lu, J. Paulk, P. McCarren, F. F. Wagner, D. Barker, E. Howe, F. Lazzaro, J. P. Gale, Y.-L. Zhang, A. Subramanian, C. A. Fierke, S. A. Carr, E. B. Holson, *ACS Chem. Biol.* **2014**, *9*, 2210–2216.
- [7] Y. Qian, J. Zhang, Y.-S. Jung, X. Chen, *PLoS One* **2014**, *9*, e84015.
- [8] C. Schölz, B. T. Weinert, S. A. Wagner, P. Beli, Y. Miyake, J. Qi, L. J. Jensen, W. Streicher, A. R. McCarthy, N. J. Westwood, S. Lain, J. Cox, P. Matthias, M. Mann, J. E. Bradner, C. Choudhary, *Nat. Biotechnol.* **2015**, *33*, 415–423.
- [9] T. B. Toro, T. J. Watt, *Protein Sci.* **2015**, *24*, 2020–2032.
- [10] B. J. Wilson, A. M. Tremblay, G. Deblois, G. Sylvain-Drolet, V. Giguère, *Mol. Endocrinol.* **2010**, *24*, 1349–1358.
- [11] N. A. Wolfson, C. A. Pitcairn, C. A. Fierke, *Biopolymers* **2013**, *99*, 112–126.
- [12] I. Rettig, E. Koeneke, F. Trippel, W. C. Mueller, J. Burhenne, A. Kopp-Schneider, J. Fabian, A. Schober, U. Fernekorn, A. von Deimling, H. E. Deubzer, T. Milde, O. Witt, I. Oehme, *Cell Death Dis.* **2015**, *6*, e1657.
- [13] S. Y. Park, J. A. Jun, K. J. Jeong, H. J. Heo, J. S. Sohn, H. Y. Lee, C. G. Park, J. Kang, *Oncol. Rep.* **2011**, *25*, 1677–1681.
- [14] I. Oehme, H. E. Deubzer, D. Wegener, D. Pickert, J.-P. Linke, B. Hero, A. Kopp-Schneider, F. Westermann, S. M. Ulrich, A. von Deimling, M. Fischer, O. Witt, *Clin. Cancer Res.* **2009**, *15*, 91–99.
- [15] G. Niegisch, J. Knievel, A. Koch, C. Hader, U. Fischer, P. Albers, W. A. Schulz, *Urol. Oncol.* **2013**, *31*, 1770–1779.
- [16] G. Lopez, K. L. J. Bill, H. K. Bid, D. Braggio, D. Constantino, B. Prudner, A. Zewdu, K. Batte, D. Lev, R. E. Pollock, *PLoS One* **2015**, *10*, e0133302.
- [17] A. Chakrabarti, J. Melesina, F. R. Kolbinger, I. Oehme, J. Senger, O. Witt, W. Sippl, M. Jung, *Future Med. Chem.* **2016**, *8*, 1609–1634.
- [18] S. Balasubramanian, J. Ramos, W. Luo, M. Sirisawad, E. Verner, J. J. Buggy, *Leukemia* **2008**, *22*, 1026–1034.
- [19] A. Kleinschek, C. Meyners, E. Digiorgio, C. Brancolini, F.-J. Meyer-Almes, *ChemMedChem* **2016**, *11*, 2598–2606.
- [20] M. Muth, N. Jänsch, A. Koprancovic, A. Krämer, N. Wössner, M. Jung, F. Kirschhöfer, G. Brenner-Weiss, F.-J. Meyer-Almes, *General Subj.* **2019**, *1863*, 577–585.
- [21] N. Jänsch, C. Meyners, M. Muth, A. Koprancovic, O. Witt, I. Oehme, F.-J. Meyer-Almes, *Redox Rep.* **2019**, *20*, 60–67.
- [22] C. Mathieu, R. Duval, A. Cocaign, E. Petit, L.-C. Bui, I. Haddad, J. Vinh, C. Etchebest, J.-M. Dupret, F. Rodrigues-Lima, *J. Biol. Chem.* **2016**, *291*, 23842–23853.
- [23] C. Mathieu, L.-C. Bui, E. Petit, I. Haddad, O. Agbulut, J. Vinh, J.-M. Dupret, F. Rodrigues-Lima, *J. Biol. Chem.* **2017**, *292*, 1603–1612.
- [24] J. Fuhrmann, V. Subramanian, P. R. Thompson, *ACS Chem. Biol.* **2013**, *8*, 2024–2032.
- [25] M. Yang, Z. Liu, C. Hughes, A. M. Stern, H. Wang, Z. Zhong, B. Kan, W. Fenical, J. Zhu, *Proc. Natl. Acad. Sci. USA* **2013**, *110*, 2348–2353.

Manuscript received: April 8, 2020

Revised manuscript received: May 11, 2020

Accepted manuscript online: May 19, 2020

Version of record online: September 11, 2020